The Active Site of Hemerythrin As Determined by X-ray Absorption Fine Structure†

Ke Zhang,‡ E. A. Stern,* and F. Ellis§
Department of Physics, FM-15, University of Washington, Seattle, Washington 98195
J. Sanders-Loehr and A. K. Shiemke∥
Department of Chemical and Biological Sciences, Oregon Graduate Center, Beaverton, Oregon 97006-1999
Received December 10, 1987; Revised Manuscript Received May 25, 1988

ABSTRACT: Extensive X-ray absorption fine structure measurements and analysis have been made on azidomet- and methemerythrin and on the native forms of oxy- and deoxyhemerythrin. Due to the availability of models that have been synthesized to mimic the active site of hemerythrin, it was possible to make a thorough assessment of the various errors in the structural parameters determined by the analysis. It is found that the largest source of error is the lack of complete transferability of amplitude and phase between the standards and hemerythrin. This is of particular importance in distinguishing the contributions of the second-shell low-Z atoms and, thus, has a substantial influence on the determination of the iron–iron distance. The internal consistencies of the various checks and a new formulation of error analysis for the structural parameters give us confidence in the structure determined for the active site. The main result is that as O_2 is released from oxyhemerythrin, the μ-oxo bridge between the two iron atoms in the active site with an Fe–O distance of 1.8 Å converts to a μ-hydroxo bridge in deoxyhemerythrin, expanding the Fe–O distance to 2.0 Å. The Fe–Fe distance expands proportionally from 3.24 Å in oxyhemerythrin to 3.57 Å in deoxyhemerythrin so as to keep the Fe–O–Fe bridging angle approximately constant. These conclusions provide experimental support for the structures of oxy- and deoxyhemerythrin proposed previously on the basis of spectroscopic and preliminary X-ray crystallographic data.

Hemerythrin (Hr) is an oxygen-transport protein found in a number of marine invertebrates. The active site of the protein contains two non-heme iron atoms and reversibly binds one molecule of oxygen. Prolonged exposure to anions such as azide or hydroxide or to oxidants such as ferricyanide leads to methemerythrin in which the peroxide is replaced or removed. Mössbauer, magnetic susceptibility, and X-ray absorption spectroscopy measurements have established that the iron atoms are in the ferrous state in the deoxy form and in the antiferromagnetically coupled ferric state in the oxy and met forms (Loehr & Loehr, 1979; Wilkins & Harrington, 1983).

The structure of hemerythrin has been investigated by X-ray crystallography for more than a decade, although the studies have mainly been on the met forms and not on the physiologically more interesting deoxy- and oxyhemerythrin, due to the instability of these forms (Stenkamp & Jensen, 1979; Stenkamp et al., 1984; Sheriff et al., 1987). The structure of the binuclear iron site in azidomethemerythrin consists of two hexacoordinate iron atoms ligated to the protein by five histidines, two bidentate carboxylate bridges, and a μ-oxo bridge between the iron atoms (Stenkamp et al., 1984). A recent crystallographic study on oxy- and deoxyhemerythrin indicated that dioxygen binds in the same location as azide, resulting in the structures shown in Figure 1 (Stenkamp et al., 1985). Although the resolution for the deoxy form was considerably poorer, the coordination number of the iron atoms appeared to be pentacoordinate for one iron and hexacoordinate for the other. According to this model, there is a hydroxo bridge in deoxyhemerythrin which, when dioxygen binds, donates a proton to the incipient peroxide anion. The μ-oxo bridge in oxyhemerythrin then behaves as a hydrogen bond acceptor, thereby stabilizing the bound hydroperoxide. A hydroxo-bridged structure in deoxyhemerythrin is supported by magnetic circular dichroism and NMR experiments (Reem & Solomon, 1987; Maroney et al., 1986). A hydrogen-bonded structure in oxyhemerythrin is supported by X-ray crystallographic and resonance Raman spectroscopy results (Stenkamp et al., 1985; Shiemke et al., 1986). However, this evidence is still ambiguous and deserves further investigation.

Extended X-ray absorption fine structure (EXAFS) is an advantageous technique for studying the active site because it can focus on the binuclear iron environment, even for the protein in solution, and can probe the native forms in addition to the met forms. By directly analyzing the fine structure caused by backscattering of the X-ray-excited photoelectron on neighboring atoms, it can give radial interatomic distances, the number and types of ligands around the absorbing atom, and the relative Debye–Waller factor between center and neighboring atoms in the radial direction (Stern, 1974; Stern & Heald, 1983; Stern et al., 1975).

Previous EXAFS studies on hemerythrin have shown that the active site structure is very similar in the oxy and met forms and that the short μ-oxo bridge between the Fe atoms disappears in the deoxy form (Elam et al., 1982, 1983; Co, 1983). However, the distance determination for azido- and methydroxohemerythrin from our previous EXAFS studies gave an anomalously large Fe–Fe value compared with the X-ray crystallographic results. In the present work further EXAFS experiments have been performed to gain additional information about the structure of the binuclear iron center in

† The research reported here was supported by the National Science Foundation (PCM-82-04234), the National Institutes of Health (GM 18865), and the U.S. Department of Energy on a subcontract from North Carolina State University (DE-A505-80ER10742).
‡ Present address: Institute for Structural and Functional Studies, 3401 Market St., No. 320, Philadelphia, PA 19104.
§ Present address: Wesleyan University, Middletown, Connecticut 06457.
∥ Present address: University of Georgia, Athens, GA 30602.

0006-2960/88/0427-7470$01.50/0

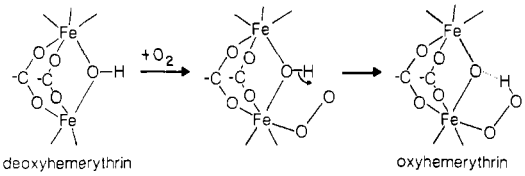

FIGURE 1: Proposed active site structures and pathway for reversible oxygen binding to hemerythrin (Stenkamp et al., 1985).

various forms of hemerythrin. Of particular assistance in this regard has been the availability of synthetic models that mimic the iron coordination geometry in hemerythrin (Hedman et al., 1986). The compound (FeOFe)(Bpz), containing a binuclear iron site bridged by a μ-oxo atom and two pairs of carboxyl oxygens with pyrazole rings as the other ligands, best approximates the active site of the met and oxy forms of hemerythrin (Armstrong et al., 1984). The compound (FeOFe)(tacn) has the same type of first-neighbor atoms as (FeOFe)(Bpz) except that the nitrogen atoms are saturated (Wieghardt et al., 1985). The compound (FeOHFe)(Bpz) has a similar environment as (FeOFe)(Bpz), except that the μ-oxo bridge is replaced by a μ-OH bridge (Armstrong & Lippard, 1984) and therefore approximates the active site of deoxy-Hr. Use of these model compounds as standards as well as careful error analysis has helped to resolve the previously observed discrepancies between EXAFS and X-ray crystallographic results.

Experimental Procedures

Hemerythrin. Hemerythrin samples from the sipunculid *Phascolopsis gouldii* were prepared and measured as described previously (Elam et al., 1982, 1983). Oxy- and deoxyhemerythrin samples were 20 mM in iron and were dissolved in 0.05 M Tris and 0.2 M sulfate (pH 8.0). Methemerythrin (22 mM in Fe) was in 0.05 M MES and 0.1 M Na_2SO_4 (pH 6.2). Azidomethemerythrin (28 mM in Fe) was in 0.1 M Tris–sulfate and 0.01 M NaN_3 (pH 7.5).

Standard Compounds. Several standard compounds were used in the study. We list them and their abbreviations as used in this paper: $[Fe_3O(glycinato)_6(H_2O)_3](ClO_4)_7$ as (Fe_3O)(Gly), [Fe(II)bis(acetonitrile)(2,3,9,10-tetramethyl-1,4,8,11-tetrazacyclotetradeca-1,3,8,10-tetraene)]PF_6 as Fe(TIM), iron(II) hexafluorophosphate, $[Fe_2O(triazacyclononane)_2(OAc)_2]I_2 \cdot 3H_2O \cdot {}^1/_2NaI$ as (FeOFe)(tacn), $[Fe_2O$-[tris(1-pyrazolyl)borate]$_2(OAc)_2] \cdot {}^1/_2CH_3CN$ as (FeOFe)-(Bpz), and $[Fe_2OH$[tris(1-pyrazolyl)borate]$_2(OAc)_2]$-$(ClO_4) \cdot 0.5CH_2Cl_2$ as (FeOHFe)(Bpz),

The (Fe_3O)(Gly) trimer was prepared and characterized as described previously (Heald et al., 1979). The Fe(TIM) compound was supplied and characterized by Dr. Norman Rose. The oxo-bridged Fe(Bpz) dimer was prepared by Dr. William D. Wheeler according to the procedure of Armstrong et al. (1984). The hydroxo-bridged Fe(Bpz) dimer was the gift of Dr. Stephen J. Lippard. The oxo-bridged Fe(tacn) dimer (Wieghardt et al., 1985) was provided by Dr. Karl Wieghardt.

EXAFS Measurements. Measurements were performed on all forms of Hr and on the standards at the Stanford Synchrotron Radiation Laboratory (SSRL) on beamlines 4-1 and 4-2 under dedicated running conditions. Measurements on azidomethemerythrin and the standard (FeOHFe)(Bpz) were also obtained at beamline X-11 at the National Synchrotron Light Source (NSLS). The measurements were made from 30 K to room temperature.

The X-ray absorption of the hemerythrin samples was monitored by fluorescence, using an ion chamber as detector and a manganese X-ray filter and soller slit assembly (Stern & Heald, 1983). The samples were contained in Teflon cells with Kapton windows. Low-temperature measurements were made by using a Displex refrigerator after the samples had been rapidly cooled by dipping into liquid nitrogen to produce fine crystallites and to minimize Bragg peaks, which distort the EXAFS background. A series of scans were collected, for a total signal of 1×10^7 counts per point for the data taken early in the collecting period and 2×10^7 counts per point for later data. The model compounds were measured as powdered solids in transmission and have a much better signal to noise ratio.

No radiation damage to the samples was detected in exposure to the X-rays. This was determined several ways. No detectable difference of the X-ray absorption spectrum of the protein occurred between the first and last scans. The methemerythrin and oxyhemerythrin samples exhibited their normal color before and immediately after being measured, while the deoxyhemerythrin sample remained colorless except for some oxidized red color on the cell edge after the run, a region that had not been exposed to X-rays. Subsequent analysis of the optical absorption spectra of these samples a few days after the run showed that the deoxy sample maintained 95% deoxy, with about 5% of the protein denatured. The oxy sample had about 10% of the protein denatured, and 20% of it was oxidized to met form. Most of the denaturation and oxidation probably occurred after the sample was measured, during the several days that the protein was thawed before the optical spectra were taken.

Data Analysis and Results

The standard EXAFS formula for the K-edge and single scattering is given by (Stern, 1974)

$$\chi(k) = \sum_j \frac{N_i B_j(k)}{R_j^2} \exp\left(\frac{-2R_j}{\lambda}\right) \sin\left[2kR_j + \delta_j(k)\right] \exp(-2k^2\sigma_j^2) \quad (1)$$

The sum is over coordination shells at average distance R_j relative to the center atom with N_j atoms in the shell. The photoelectron wave number k is defined by

$$\hbar^2k^2/2m = E - E_0$$

where E_0 is the binding energy; E is the photon energy; $B_j(k)$ and $\delta_j(k)$, both dependent on the type of scatterer, are the backscattering amplitude and phase shift, respectively; λ is the mean free path, to account for the finite lifetime of the photoelectron; and σ_j is the root-mean-square variation of the atom distance about is mean distance R_j, caused by structural or thermal effects. In EXAFS the Debye–Waller factor, $\exp(-2k^2\sigma_j^2)$, is a valid approximation for small enough values of σ or for Gaussian disorder. The analysis was done on samples measured at 80 K and at room temperature.

The analysis of the EXAFS follows standard procedures described elsewhere (Stern, 1974; Stern & Heald, 1983; Stern et al., 1975) and summarized here. The oscillatory EXAFS data were obtained by subtracting the slowly varying atomic absorption spectra background and normalizing by the edge step. Converting energy to wave number k gives the $\chi(k)$ function. The χ data for different forms of hemerythrin and model compounds are shown in Figure 2. A Fourier transform was performed with respect to k to obtain an atom distribution function with respect to the radial distance R around the central atom, as shown in Figure 3 for azidomethemerythrin. An isolated single-shell $\chi(k)$ is obtained by back-transforming

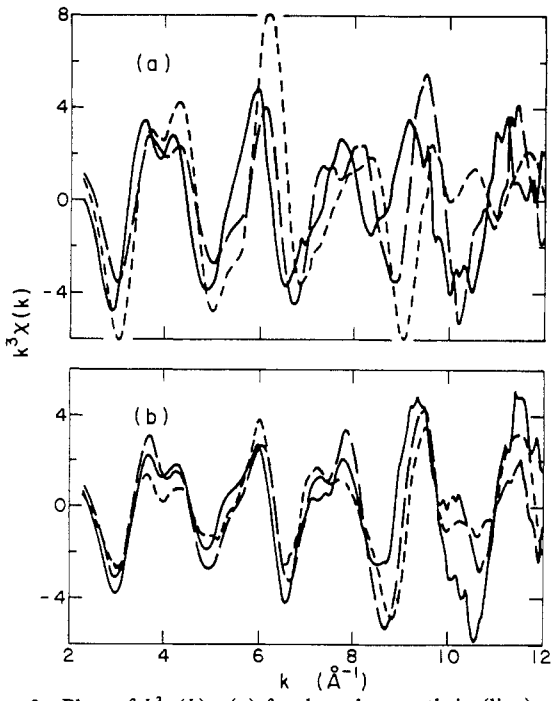

FIGURE 2: Plots of $k^3\chi(k)$: (a) for deoxyhemerythrin (line), methemerythrin (long dash), and (FeOHFe)(Bpz) (short dash); (b) for oxyhemerythrin (line), azidomethemerythrin (long dash), and (FeOFe)(Bpz) (short dash). All data taken at 80 K.

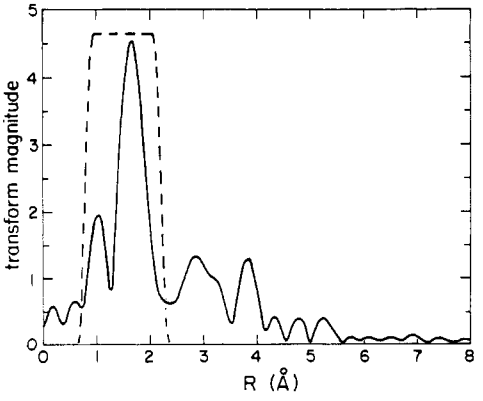

FIGURE 3: Magnitude of the transform of $k^3\chi(k)$ for azidomethemerythrin over the range $3.2 \leq k \leq 11.0$ Å^{-1}, taken at 80 K. The window function used to isolate the first shell is also shown. It has a half-width of 0.8–2.2 Å.

a single-shell signal from R-space back to k-space by using the window function shown in Figure 3 for the first shell of azidomethemerythrin.

First Shell. Since the first shell of hemerythrin is a mixture of oxygen and nitrogen with several different distances, the ratio method (Stern & Heald, 1983; Stern et al., 1975) is not appropriate. A nonlinear least-squares fitting technique was used which fits the back-transform of the first-shell $\chi(k)$ data by using $B(k)$, $\delta(k)$ from standards. The typical window size used for the back-transform was from 0.8 to 2.2 Å (Figure 3). Similar windows were used for the standards to compensate for window distortion effects. (Fe_3O)(Gly) with all oxygens in the first shell of iron was selected as an oxygen standard, and Fe(TIM) was selected as a nitrogen standard. Guided by the X-ray results (Stenkamp et al., 1984), the first shell of the oxy and met forms of hemerythrin was modeled by a single μ-oxo-bridged oxygen, a second subshell of oxygen, and a subshell of nitrogen, modified by Debye–Waller factors to allow for a spread in the distances about the mean. The program was then allowed to vary the three distances, the three

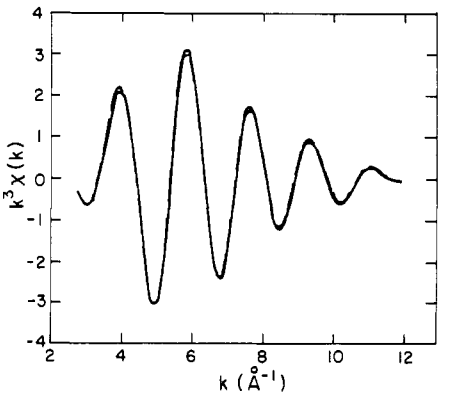

FIGURE 4: Isolated first shell of $k^3\chi(k)$ for deoxyhemerythrin (solid) and the fit (dashed).

Table I: Results of Fits to the EXAFS for the First Coordination Shell[a]

	bridging O		oxygen		nitrogen	
sample	no.	R (Å)	no.	R (Å)	no.	R (Å)
(FeOFe)-(tacn)	1.0 (3)	1.81 (3)	2.0 (4)	2.04 (4)	3.0 (5)	2.18 (4)
(FeOFe)-(Bpz)	1.0 (3)	1.80 (3)	2.0 (4)	2.04 (4)	3.0 (5)	2.16 (4)
(FeOHFe)-(Bpz)	1.0 (3)	1.98 (4)	2.0 (4)	2.00 (4)	3.0 (5)	2.12 (4)
azidometHr	1.0 (3)	1.80 (3)	2.0 (4)	2.08 (4)	3.0 (5)	2.17 (4)
metHr	1.0 (3)	1.82 (3)	2.0 (4)	2.07 (4)	2.5 (5)	2.14 (4)

	bridging O		O or N[b]		O or N[b]	
	no.	R (Å)	no.	R (Å)	no.	R (Å)
oxyHr	1.0 (4)	1.82 (3)	2.5 (5)	2.11 (4)	2.5 (6)	2.22 (4)
deoxyHr	1.0 (4)	1.98 (4)	2.4 (6)	2.12 (6)	2.5 (6)	2.25 (6)

[a] (Fe_3O)(Gly) and Fe(TIM) used as standards. All numbers of first-shell atoms are per Fe atom. The uncertainty in the value of the last digit is shown in parentheses. The fittings were done for low-temperature data (80 K or lower). The differences in DWF's are close to zero and are not listed. [b] Contributions of oxygen and nitrogen atoms cannot be distinguished.

Debye–Waller factors, and the three coordination numbers to obtain the best fit in both phase and amplitude between the manufactured signal and the hemerythrin first-shell data. E_0 was not a variable but was set as discussed in the Appendix. (Fe_3O)(Gly), which was used as the oxygen standard, contains six oxygens in its first shell, with an average distance of R = 2.02 Å. Fe(TIM), the nitrogen standard, contains six nitrogens in its first shell at an average distance of R = 1.94 Å. Both of these standards had their $B(k)$ corrected for their structural Debye–Waller factors, and data taken at 80 K were employed. Figure 4 shows the agreement achieved between deoxyhemerythrin first-shell data and fit. The fit for oxyhemerythrin is similar. Table I lists the results of the fit and their errors, which were determined as discussed in the Appendix. For the model compounds and the azidomet and met forms of hemerythrin, it was possible to distinguish between the nitrogen and the oxygen atoms on the basis of their significant differences in bond length. However, for the oxy and deoxy forms of hemerythrin listed in Table I this distinction was not possible within the uncertainties.

However, close agreement between the fit and the data does not in itself guarantee reliable values of the fitting parameters; a careful error analysis is necessary. As described in the Appendix, the major contribution to the error in the fitting parameters is the lack of complete transferability of the EXAFS amplitude and phase between the standards and the hemerythrin. To improve the transferability of amplitude and phase requires standards that have an iron environment closer

Table II: Fits of the Difference in the First-Shell EXAFS

	deoxyHr minus oxyHr[a]				azidometHr minus (FeOFe)(Bpz)[b]			
type of atom	no.	R (Å)	no.	R (Å)	no.	R (Å)	no.	R (Å)
μ-oxo	1.0 (3)	1.98 (3)	1	1.82	1	1.82 (3)	1	1.79
O or N	2.5 (4)	2.13 (5)	2.5	2.11	2	2.06 (3)	2	2.04
O or N	2.3 (4)	2.24 (5)	2.5	2.22	3	2.18 (4)	3	2.17

[a] First two columns were obtained for deoxyhemerythrin by assuming the values for oxyhemerythrin given in the second two columns. [b] Analysis for azidomethemerythrin and the (FeOFe)(Bpz) model similar to that in footnote *a*.

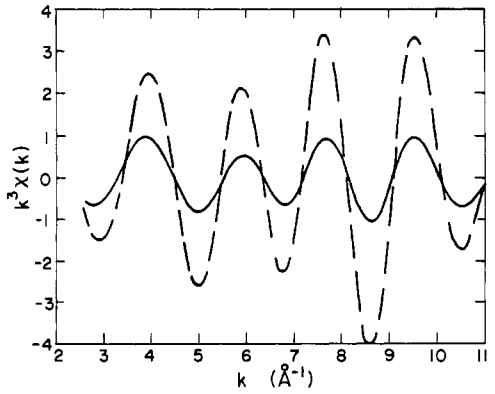

FIGURE 5: Difference in the first-shell $k^3\chi(k)$ between azidomethemerythrin and (FeOFe)(Bpz) (solid) compared with the $k^3\chi(k)$ of azidomethemerythrin (dashed).

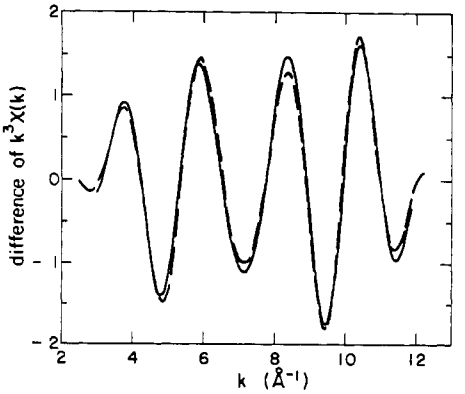

FIGURE 6: Fit (dash) of the difference in the first-shell $k^3\chi(k)$ between deoxyhemerythrin and oxyhemerythrin (solid).

to the unknown. The model compounds (FeOFe)(Bpz) and (FeOFe)(tacn) better approximate the active site of the oxy and met forms of hemerythrin, while (FeOHFe)(Bpz) is a better approximation of the active site of deoxyhemerythrin than the standards employed, even though it is a ferric complex while deoxyHr is a ferrous one. The problem with using these models as standards is that their first shell is a mixture of various distances of oxygen and nitrogen atoms and it is not possible to separate out uniquely each contribution. The standards (Fe_3O)(Gly) and Fe(TIM) were chosen because only one type of atom contributes in each case, but consequently they do not closely approximate the active site.

One way around this dilemma is to take the difference between the model and the hemerythrin. If they are truly similar, then their isolated first-shell difference should be much smaller than either isolated $\chi(k)$. As an example, if the model has exactly the same environment as the unknown, the difference between them is zero and the structure of the unknown is the same as the model with uncertainties determined by only the measurement noise in the data, with no contributions from the inadequacies of the standard.

Several χ data differences between various forms of hemerythrin and between hemerythrin and model compounds were taken, and their first shells were isolated by back Fourier transform. Only the difference between azidomethemerythrin and (FeOFe)(Bpz) was small enough to indicate a close similarity in first-shell environments. These data are shown in Figure 5 and enumerated in Table II. The fit to the difference between deoxy- and oxyhemerythrin is shown in Figure 6. The results of the fits are given in Table II. Note that the uncertainties are smaller than the corresponding ones in Table I. In particular, the uncertainty in the coordination of the bridging oxygen is now small enough to distinguish between the values of 1 or 0.5. Thus, it is important in interpreting the change in the bridging oxygen as O_2 is released. The μ-oxo bridge, which contributes one oxygen per iron at an average distance of 1.82 Å in oxyhemerythrin, is replaced by one oxygen per iron at 1.98 Å in deoxyhemerythrin. This allows us to rule out the possibility of breaking the bridge in deoxyhemerythrin with the oxygen remaining attached to only one Fe atom to give a coordination number of 0.5. Moreover, the alternative of replacing the μ-oxo bridge in oxyhemerythrin with a μ-hydroxo bridge in deoxyhemerythrin is consistent with the measured result of its coordination number remaining at one.

Table III: X-ray Crystallographic Results for Model Compounds and Hr

	bridging O(H)		oxygen		nitrogen		Fe
sample	no.	R (Å)	no.	R (Å)	no.	R (Å)	R (Å)
(FeOFe)(tacn)[a]	1	1.79	2	2.03	3	2.16	3.06
(FeOFe)(Bpz)[b]	1	1.79	2	2.04	3	2.17	3.15
(FeOHFe)(Bpz)[c]	1	1.96	2	2.00	3	2.10	3.44
azidometHr[d]	1	1.77	2	2.23	3	2.25	3.25
metHr[d]	1	1.80	2	2.11	2.5	2.21	3.21

[a] Wieghardt et al., 1985. [b] Armstrong et al., 1984. [c] Armstrong & Lippard, 1984. [d] Stenkamp et al., 1984.

An independent measure of the accuracy of the EXAFS results can be obtained by comparing these values with the X-ray diffraction values for the model compounds and met forms of hemerythrin, which are listed in Table III. When this comparison is made, it can be seen that the errors in the X-ray crystallography determinations for the small molecules of the models are negligible relative to the EXAFS errors. The larger errors for the hemerythrin macromolecules of ~0.1 Å reflect, in part, the lower resolution of the X-ray structures. As can be seen, the agreement is within the experimental uncertainties, giving credence to our procedure and error analysis.

The most striking result in Tables I and II is the removal of the μ-oxo bridge at 1.82 Å in oxyhemerythrin and its replacement by a new bond at 1.98 Å in deoxyhemerythrin. The length of the new bond matches the length of a hydroxo bridge, as found in the Fe(II)(me-tacn) dimer (Chaudhuri et al., 1985). It is evidence that the μ-oxo bridge in oxyhemerythrin changes to a hydroxo bridge in deoxyhemerythrin. The other bonds in the first shell do not change significantly. In the case of oxy- and deoxyhemerythrin we cannot distinguish between oxygen and nitrogen. Both fits are acceptable by interchanging nitrogen and oxygen to longer or shorter bonds. However,

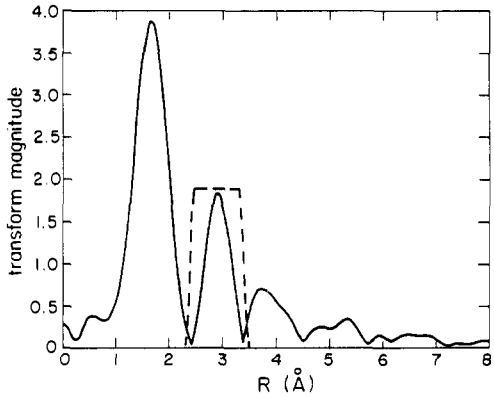

FIGURE 7: Transform of the same data as in Figure 3, but over the range $5.0 \leq k \leq 11.8$ Å^{-1}. The window used to isolate the Fe–Fe peak is shown with its half-width from 2.4 to 3.4 Å.

since oxygen atoms are the shorter bonds in azidomethemerythrin, it is reasonable to assign the shorter bond (2.13 Å) as the Fe–oxygen bond. The quality of fit for deoxyhemerythrin was not significantly different, with either hexacoordinate for both irons or one hexa and the other pentacoordinate. Thus, unfortunately, the determination of whether or not one iron is pentacoordinate is not discernible within our present experimental limitations. A pentacoordinate iron with a free site for exogenous ligand binding has been implied from spectroscopic and kinetic analysis of deoxyhemerythrin (Reem & Solomon, 1987; de Waal & Wilkins, 1976).

Second Shell. Iron–iron distances were obtained from the ratio method (Stern & Heald, 1983; Stern et al., 1975) by comparing the phase and amplitude of the χ, giving rise to the iron–iron peak with a similar signal from known compounds. For the ratio method to be accurate, the unknown and the standard should have a similar environment for the corresponding shell. For both the standards and hemerythrin, the window used to isolate the iron atoms includes some low-Z atoms (carbon, oxygen, or nitrogen), which also contribute a signal to the iron–iron shell. There is a need to separate the low-Z signal from the iron signal. In principle, the iron signal can be separated from the low-Z atoms by its different amplitude and phase dependence (Teo & Lee, 1979) with k. In particular, the Fe backscattering amplitude is larger than that of the low-Z atoms for $k \geq 5$ Å^{-1}. As a check for eliminating the low-Z signal, we transformed the data over various ranges containing increasingly higher average values of k and tried to obtain a converent result. Consistent results in the comparison between standards and Hr required using k values greater than 5 Å^{-1}. The Fourier transform for this k range and the back-transform window are shown in Figure 7.

Another check was made by taking the ln of the ratio of the amplitudes of the same compound at different temperatures. One should get a straight line in such a plot versus k^2 if there is only one kind of atom in the shell. A straight line was obtained only for the k range for the Fourier transform larger than 5 Å^{-1}, consistent with the previous result. The signal from low-Z atoms is suppressed in the high k region, due not only to its backscattering dependence but also to the large spread in distances within the window. For example, the X-ray structure determination indicates that the second shell of (FeOFe)(Bpz) contains five low-Z atoms between 2.90 and 3.40 Å with a mean-square variation σ^2 of 0.027 Å^2. At $k = 6$ Å^{-1}, the amplitude from a low-Z atom is consequently reduced by a factor of $\exp(2k^2\sigma^2) = 7$. Even then, some low-Z signal remained in the second shell data, as indicated by the fact that the ln of amplitude ratios between standard compounds with one iron neighbor and (Fe_3O)(Gly) with two iron neighbors have a larger (20%–30%) intercept at $k^2 = 0$ than they should, presumably because the former ones contained a larger proportion of low-Z signal than the latter one, giving a larger signal at lower k and artificially increasing the slope.

Table IV: Fe–Fe Distances Determined by Comparison with Suitable Standards

sample	standard	ΔE_0[a] (eV)	ΔR[b] (Å)	R (Å)
oxyHr	(FeOFe)(tacn)	4.0	0.16	3.22
	(FeOFe)(Bpz)	2.0	0.10	3.24
	metHr	2.0	0.12	3.25
	azidometHr	2.0	0.0	3.24
deoxyHr	(FeOHFe)(Bpz)	0.0	0.16	3.58
	(Fe_3O)(Gly)	4.0	0.26	3.57

[a] E_0 shift required to match the phase at $k = 0$. [b] The difference in distance between the sample and the standard.

Having a different proportion of low-Z signal or a different charge distribution about the Fe atom could also affect the relative phase between the standard and the hemerythrin. This effect can be detected by comparing the intercept at $k = 0$ of the difference in phase between standard and unknown. If this intercept is far from zero or multiples of 2π and requires a relative E_0 shift by more than a few electron volts, the standard is unreliable and can give significant errors in distance, which is determined by the slope of the phase difference plotted as a function of k.

(Fe_3O)(Gly) had been used as a standard at the initial stage of data analysis (Elam et al., 1982, 1983). Its validity for determining the iron–iron distance in hemerythrin and model compounds was tested carefully. It was found that all the phase difference plots of (FeOFe)(tacn) and (FeOFe)(Bpz), as well as oxy and met forms of hemerythrin with (Fe_3O)(Gly), did not pass through the origin as they should have, and the required E_0 shifts to do so were usually more than 10 eV. On the other hand, the correct intercept of the phase difference plot required only a few electron volts of E_0 shift if the μ-oxo-bridged binuclear complexes were used as the standard. Table IV shows the determined iron–iron distance in oxy- and deoxyhemerythrin by using various standards as well as met forms of hemerythrin.

The distance deduced from the (Fe_3O)(Gly) standard in all forms of Hr except deoxyHr was 0.2 Å longer than the results obtained by using the μ-oxo-bridged standards, and more than a 10 eV shift of E_0 was needed, compared with only a few electron volts in the μ-oxo-bridged cases (Table IV). The ratios for met forms of hemerythrin with the standards show the same story. A necessary condition of a good standard for the Fe–Fe distance of hemerythrin is that the irons have similar bridging oxygens. The importance of choosing models with appropriate Fe–O–Fe bond angles has been noted previously (Co et al., 1983). From the present work it is clear that the chemical state of the bridging oxygen and the related Fe–O bond distance can also have a marked effect. (Fe_3O)(Gly) is a poor standard for the oxy and met forms, and the Fe–Fe distance determined by its use previously (Elam et al., 1982, 1983) is in error. (FeOFe)(tacn) and (FeOFe)(Bpz) with similar μ-oxo-bridge angles are good standards for met and oxy hemerythrin. However, the μ-oxo-bridged model compounds are not good standards for the iron–iron distance in deoxyhemerythrin due to the requirement of a big E_0 shift to make the phase plot intercept at zero. Guided by the first-shell result that a hydroxo bridge in deoxyhemerythrin has replaced a μ-oxo bridge in oxyhemerythrin, (FeOHFe)(Bpz) has been used to obtain the deoxyhemerythrin Fe–Fe neighbor distance. Also, (Fe_3O)(Gly) was found to be a good standard in this case because now the short Fe–O bond has lengthened to a value

Table V: Fe–Fe Distances, Difference in σ^2 from 80 to 300 K, and Fe–O–Fe Angles As Determined by EXAFS

sample	Fe–Fe[a] (Å)	$\Delta\sigma^2$ ($\times 10^{-3}$ Å^2)[b]	Fe–O–Fe angle (deg)[c]
(FeOFe)(Bpz)	3.14 (4)	1.5 (4)	121
(FeOHFe)(Bpz)	3.42 (5)	2.5 (4)	119
azidometHr	3.24 (5)	3.1 (5)	127
metHr	3.13 (5)	3.3 (5)	118
oxyHr	3.24 (5)	1.0 (8)	125
deoxyHr	3.57 (6)	7.0 (10)	128

[a] (FeOFe)(tacn) was used as the standard for (FeOFe)(Bpz) and azidomet- and metHr. (Fe_3O)(Gly) was used as the standard for (FeOHFe)(Bpz). The values for oxy- and deoxyhemerythrin are derived from the information in Table IV. [b] The difference in the mean-square vibrational amplitudes from 80 to 300 K. [c] Determined from Fe–Fe distance and Fe–O values in Table I and II.

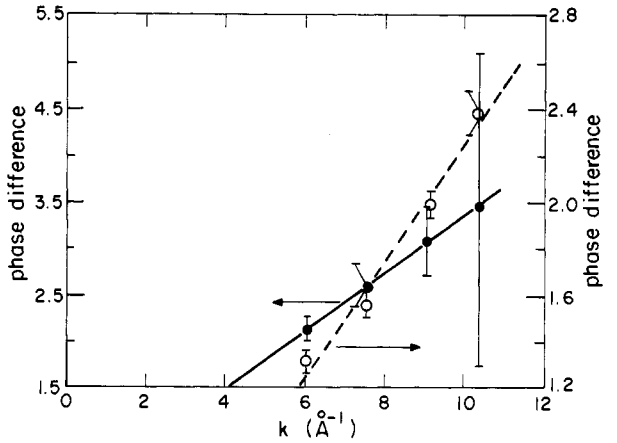

FIGURE 8: Difference in phase in the Fe–Fe shell between azidometHr and metHr at 30 K (dashed) and between deoxyHr and (FeOHFe)(Bpz) at 80 K (solid).

closer to those in this standard.

The iron–iron distances, the Debye–Waller factors (DWF), and the Fe–O–Fe angle of model compounds and hemerythrin as determined by EXAFS are summarized in Table V. The Fe–Fe distances for the various forms of hemerythrin were determined as described above. These distances in (FeOFe)(Bpz) and (FeOHFe)(Bpz) were obtained by using (FeOFe)(tacn) and (Fe_3O)(Gly) as the standards, respectively. The Fe–O–Fe angle was calculated by geometry using the EXAFS values of the Fe–O bridging distance in Tables I and II and the Fe–Fe distance of Table V. A significant difference (0.1 Å) in the iron–iron distance was found between met- and azidomethemerythrin. This difference is most clearly evident in the phase difference plot of the direct ratio between them as shown in Figure 8 (dashed line). The distance difference between deoxyhemerythrin and (FeOHFe)(Bpz) is 0.15 Å, and the phase difference plot is also shown in Figure 8 (solid line).

The increase of 0.3 Å in Fe–Fe distance between the deoxy and oxy forms reflects a significant change. Note, however, that the Fe–O–Fe angle remains approximately the same. The Fe–Fe distances are in good agrement with the values determined by X-ray crystallography (Table III), particularly for (FeOFe)(Bpz), (FeOHFe)(Bpz), and azidomethemerythrin. The smaller Fe–Fe distance and Fe–O–Fe angle for methemerythrin (Table V) show less good agreement with the X-ray crystallographic data (Table III) and with the vibrational data (Shiemke et al., 1984), which indicate similar Fe–O–Fe angles for the met and azidomet forms. The reason for this disagreement is unknown. However, using different standards and direct comparison with azidometHr all give agreement with the shorter Fe–Fe distance in metHr. Thus, we can have confidence in the Fe–Fe distances of 3.24 ± 0.05 Å for oxyhemerythrin and 3.57 ± 0.06 Å for deoxyhemerythrin based on EXAFS analysis alone.

The various forms of hemerythrin exhibit quite a different temperature dependence of the DWF of the Fe–Fe pairs. The largest DWF was found for deoxyhemerythrin, showing a weaker connection between the two irons. It is also interesting to note that the temperature dependence of the DWF of iron pairs in oxyhemerythrin is considerably smaller than that of the met forms and even the (FeOFe)(Bpz) model, suggesting the bridging mechanism in oxyhemerythrin may be different from those compounds.

Near-Edge Structure. The near-edge structure of X-ray absorption contains detailed information on the electron bonding and the charge distribution around the absorbing atom. Near-edge structures of hemerythrins have been published previously (Elam et al., 1982, 1983; Co, 1983). All the compounds in which the irons are in the ferric state have a wider peak than in deoxyhemerythrin, where the irons are in the ferrous state.

A detail of the absorption edge that has structural significance is the 3d "pip", which is the preedge bump below the edge. This feature is caused by transitions to unoccupied 3d states on the iron atom. Such transitions are formally forbidden by dipole selection rules if the Fe atoms are at a center of inversion symmetry but can occur weakly due to quadrupole transitions and are enhanced by inversion symmetry breaking effects. The lack of inversion symmetry of the iron environment allows odd parity states such as p states to hybridize with the d states, giving the enhancement. The intensities of the 3d pip relative to the height of the absorption edge were measured. (FeOHFe)(Bpz) and (FeOFe)(Bpz) both have six ligands per iron. The change from a μ-oxo bridge at 1.80 Å in (FeOFe)(Bpz) to a μ-hydroxo bridge at 1.98 Å in (FeOHFe)(Bpz) produces a more symmetric iron environment in the latter due to the nearer equality of the six metal–ligand bond lengths. The decrease of the 3d pip intensity from 11% for (FeOFe)(Bpz) to 4% of the edge step for (FeOHFe)(Bpz) is similar to that observed in other oxo-bridged iron complexes (Roe et al., 1984) and indicates the effect of this change. Second, the intensity change from methemerythrin to azidomethemerythrin is a 1% decrease in the 3d pip from 8% to 7%. From the EXAFS results above we know that the main iron environment change from the azido form to the met form is the loss of one ligand, yielding a less symmetric pentacoordinate iron in methemerythrin.

When deoxy- and oxyhemerythrin are compared, the change from a μ-oxo bridge in oxyhemerythrin to a hydroxo bridge in deoxyhemerythrin produces an intensity change in the 3d pip from 8% to 5%. If deoxyhemerythrin had two 6-coordinated iron atoms, the intensity of the 3d pip should be close to the one for (FeOHFe)(Bpz) due to the similar degree of symmetry in the iron environment. A 1% greater intensity for deoxy than for (FeOHFe)(Bpz) indicates that deoxy structure has a more asymmetric iron environment. This difference is what would be expected from one iron in deoxyhemerythrin being pentacoordinated, as in the difference between azidomet- and methemerythrin. It should be pointed out that deoxyHr is a ferrous complex while all the models and other forms of Hr are ferric. However, this difference does not invalid our conclusion that the deoxy structure has a more asymmetric iron environment. For a given asymmetric environment, changing from Fe(III) to Fe(II) will reduce the 3d pip because of the smaller number of d holes. The fact that the pip is increased for deoxy compared to the (FeOHFe)(Bpz)

model indicates that the asymmetry is actually larger than implied by the pip increase. In sum, the intensity of the 3d pip suggests that one of the irons in deoxyhemerythrin may be pentacoordinated, even though the EXAFS data do not have the resolution to make this distinction.

Discussion

Our EXAFS results for the model compounds in Tables I and V compare well with X-ray crystallographic results in Table III, giving confidence in the fitting procedure and error assessment. In these tables, our EXAFS distances for the met form of hemerythrin are compared with the protein X-ray crystallography results. Although some differences are found, they are within the uncertainties of the X-ray crystallography determination of ~0.1 Å. The crystallography results on the native oxy and deoxy forms of hemerythrin are too imprecise for comparison. Our result that one iron is pentacoordinated in metHr is consistent with the X-ray observation (Stenkamp et al., 1984).

Comparison can also be made with our previous EXAFS results (Elam et al., 1982, 1983). The agreement is within experimental error for the first shell of Hr in all forms. Our present results also show good agreement with several other EXAFS measurements for the first shells and for the iron–iron distances in methemerythrins (Co, 1983; Scarrow et al., 1987). However, our present results of an iron–iron distance of 3.24 Å in azidomethemerythrin and 3.57 Å in deoxyhemerythrin are in disagreement with our previous values of 3.49 Å in azidomethemerythrin and 3.13 Å in deoxyhemerythrin (Elam et al., 1982, 1983). The explanation of the discrepancies is in the standards used. The standard for the second shell used in the previous analysis was (Fe_3O)(Gly) for all forms of Hr. The present analysis shows that (Fe_3O)(Gly) is a poor standard for the met and oxy forms of hemerythrin, due to the nonsimilarity of the atom bridging the irons. Moreover, the k range of the data analysis in the previous study was from 3 to 10 $Å^{-1}$, and the contribution of low-Z atoms in the small k region would remain a significant portion of the total signal, distorting the phase difference and ln of ratio plots. This phenomenon has been amply documented in a previous EXAFS study on binuclear iron complexes (Hedman et al., 1986). The present analysis uses appropriate standards and chooses the correct k range to eliminate distortions introduced by low-Z atoms.

The standard (FeOHFe)(Bpz) used for the ferrous irons in deoxyhemerythrin had a correct hydroxo bridge, but it contained ferric irons. However, the E_0 shift needed to correct for this difference was small enough not to have introduced serious errors. The other previously reported iron–iron distance of 3.26 Å for deoxyhemerythrin (Co, 1983) appears to be in error due to the use of a μ-oxo-bridged standard instead of an FeOH-containing model compound.

An EXAFS measurement on the model compounds (FeOFe)(tacn), (FeOFe)(Bpz), and (FeOHFe)(Bpz) was reported recently (Hedman et al., 1986). A severe interference of low-Z atoms at about the same distance as iron was found. This observation is similar to ours. With the more appropriate models they obtained an iron–iron distance of 3.20 Å for azidomethemerythrin, which is also shorter than the value of 3.38 Å that they determined previously (Hendrickson et al., 1982). Although different methods for data analysis were used, the present results from the two laboratories are in good agreement with one another and with the Fe–Fe value of 3.19 Å for azidomethemerythrin recently reported by Scarrow et al. (1987).

Our current analysis of the nature of the binuclear iron center in hemerythrin gives a more explicit picture of the structural changes that accompany oxygen transport. The occurrence of a μ-oxo bridge in the azidomet and met forms of hemerythrin has been firmly established by X-ray crystallography (Stenkamp et al., 1984). The presence of a similar oxo-bridged structure in oxyhemerythrin has been strongly implied from spectroscopic measurements, particularly resonance Raman spectroscopy (Shiemke et al., 1984), and from the degree of antiferromagnetic coupling between the iron atoms (Maroney et al., 1986; Dawson et al., 1973). Our EXAFS data on oxyhemerythrin provide definitive evidence for this assignment. The conversion of the μ-oxo bridge in oxyhemerythrin to a μ-hydroxo bridge in deoxyhemerythrin has been implicated from the weakness of the iron–iron interaction in deoxyhemerythrin (Reem & Solomon, 1987; Maroney et al., 1986). The present EXAFS results on the lengthening of the Fe–O (bridge) bond and the greater temperature dependence of the Fe–Fe interaction in deoxyhemerythrin provide strong evidence for a hydroxo-bridged structure in deoxyhemerythrin. It has been proposed that a hydrogen bond may be formed in oxyhemerythrin on the oxo group from the proton which stabilizes the peroxide. This hydrogen bond would reduce the thermal vibration for iron pairs. The small DWF obtained for iron–iron atoms in oxyhemerythrin is consistent with this picture.

The measurement of the kinetics for oxygen binding to deoxyhemerythrin suggests a process that is close to diffusion controlled, thereby implying that the coordination position for oxygen binding is initially unoccupied or occupied by a weakly held group (Petrou, 1981). Due to the experimental error of our EXAFS measurements we could not decide whether one of the irons in deoxyhemerythrin is pentacoordinate. We could fit the χ data equally well for 6 or 5.5 average coordination numbers in the first shell. However, the measurement of the 3d pip did indicate that one of the irons in deoxyhemerythrin may be pentacoordinated.

In conclusion, our results support the hypothesis that a hydroxyl ion is the bridging group in deoxyhemerythrin and that this group provides a proton to the incoming dioxygen, thereby facilitating its reduction to hydroperoxide and leaving a μ-oxo bridge between the iron atoms in oxyhemerythrin (Stenkamp et al., 1985). This proton is returned to the oxo bridge when the peroxide is reoxidized and released as dioxygen, as in the formation of deoxyhemerythrin, but not when the peroxide is displaced by other anions, as in the formation of methemerythrins.

Acknowledgments

We are most grateful to Drs. Norman Rose, Stephen J. Lippard, and Karl Wieghardt for supplying the various standard compounds that made this study possible. The support and help of the staff of the Stanford Synchrotron Radiation Laboratory (SSRL) and the staff of the National Synchrotron Light Source (NSLS) were essential in conducting the experiments. SSRL and NSLS are supported by the U.S. Department of Energy.

Appendix

Error Analysis. In interpreting the results of the EXAFS analysis, the question arises of how unique is the model used for fitting the data. For example, is one of the iron atoms pentacoordinated in deoxyhemerythrin? How certain is the conclusion that the μ-oxo bridge is replaced by a μ-OH as the O_2 is released? The answers to such questions depend on the assessment of the errors in the parameters of the models used to fit the data. The discussion of such errors in the literature is inadequate. In this section we present a discussion that we

feel addresses this point adequately for the first time.

There are three types of errors. The first one is in the data themselves. Random errors are due to shot noise from the limited statistics of the numbers of X-ray photons detected and noise in the X-ray source and in the electronics. By appropriate design of the apparatus, the noise in the X-ray source and in the electronics can be minimized so that the shot noise dominates.

Systematic errors are introduced by "glitches" from the monochromator, variation of harmonic content in the X-ray beam with energy and time, inhomogeneity in the sample, and sample contamination. The sample contamination problem is particularly acute for the Fe edge because of the possibility of iron particles from tweezers or knives that may have been used to handle and manipulate the samples. Again, these errors can be minimized by proper experimental techniques.

The second type is the systematic errors introduced by the data analysis. The EXAFS has to be separated from the atomic absorption background. For most atoms this atomic background is unknown. It is assumed that it is slowly varying and separated out by a fitting routine that eliminates the slowly varying background. This assumption is not strictly correct, particularly near the edge, and introduces some systematic errors, particularly at small R values in the radial structure function determined by Fourier transforming $\chi(k)$. Other systematic errors are introduced when isolating a particular coordination shell in R-space from the rest of the spectrum. Each coordination shell is not completely separated from its neighbors, and the window function used to attempt to separate it is a compromise to include as much of the shell as possible without overlapping significantly with neighboring ones. Analysis techniques are employed to minimize these systematic errors, but they cannot be eliminated entirely.

The third type of error is one usually neglected in the literature, namely, errors in $B_i(k)$, λ, and $\delta_i(k)$ of eq 1 introduced by the standard. There is prevalent a false impression that $B_i(k)$, λ, and $\delta_i(k)$ are transferable and that knowledge of their values from theory or by comparison with standard compounds assures that no errors are introduced in the final result. These quantities are not absolutely transferable, and they depend somewhat on the local environment (Stern et al., 1980; Bunker & Stern, 1983). The closer the environment of the standards is to that of the unknown, the more accurate are the values of these parameters.

In our discussion in this Appendix we explain how we estimate each type of error. Once these errors are determined, the next question to be addressed is how many structural parameters can be determined, and with what accuracy, in view of the values of the the three types of errors discussed above.

In isolating a particular coordination shell, by necessity, a finite range in R-space is employed, the so-called window function about the coordination shell. The window range ΔR determines the spacing between k values, Δk, wherein variations in k-space of the amplitude and phase of $\chi(k)$ can occur.

The relation that has been employed for EXAFS is (Lee et al., 1981)

$$\Delta k \Delta R = \pi/2 \tag{A1}$$

As an example, consider a very narrow window ΔR about R_0 such that Δk is greater than the range of k covered by the data. Then the back Fourier transform has the form

$$A \sin (kR_0 + \phi) \tag{A2}$$

where A and ϕ are constants over the data range. As ΔR is increased so that Δk becomes smaller than the data range, A and ϕ will become functions of k with a resolution of Δk; i.e., variations in k more rapid than Δk will not be discernible. Note that for each independent value of k the data determine two functions, namely, A and ϕ. Therefore, if the data are taken over a range δk, the numbers of independent k values are

$$N = \delta k/\Delta k = (2/\pi)\delta k \Delta R \tag{A3}$$

When a modeling is done to fit the experimental data in a given coordination shell and P parameters are varied to optimize the fit, the standard theory of goodness of fit sets a requirement that the fit is satisfactory when the reduced χ^2, χ_ν^2, is less than unity (Bevington, 1969):

$$\chi_\nu^2 = \frac{1}{\nu}\left[\sum_i \frac{(\phi^i_f - \phi^i)^2}{(\sigma^i_\phi)^2} + \sum_i \frac{(A^i_f - A^i)^2}{(\sigma^i_A)^2}\right] \tag{A4}$$

Here ϕ^i and A^i are the values determined from the data at the independent point k^i, and ϕ^i_f and A^i_f are the corresponding values modeled from the standards. The rms errors in the experimental phase and amplitude introduced by the three types of contributions discussed above are denoted by σ^i_ϕ for the phase and σ^i_A for the amplitude.

The quantity

$$\nu = 2(N - P) \tag{A5}$$

is the degrees of freedom corresponding to the remaining independent variables left to determine the P parameters. The factor of 2 accounts for the fact that, at each ith point, there is both an amplitude and a phase to be fit. It follows that $P < N$ in order to assess errors in the P fitting parameters. The criterion employed to obtain the error is to vary one of the parameters, keeping all others constant so that χ_ν^2 changes from its minimum by 1. In that case the changes between the fit and the data are of the order of the rms error per degree of freedom. This assumes that all parameters are uncorrelated with one another. If this is not the case, then it is possible to find a new set of uncorrelated parameters which are linear combinations of the old parameters.

In our error analysis for the *first shell* of Hr we simplified the procedure by limiting the k range employed so that the $(\sigma^i)^2$ are all approximately the same for each independent point. In practice this requires dropping the high k portion of the data range above $k \approx 10.9$ Å^{-1}, so the k range employed was $2.5 \leq k \leq 10.9$ or $\delta k = 8.4$ Å^{-1}. The ΔR window used was $\Delta R = 1.3$ Å, so that $N = 7$ from eq A3. The EXAFS amplitude and phase are defined by setting

$$\chi(k) = A(k) \sin \phi(k) \tag{A6}$$

where $\phi(k)$ is the argument of the sine function in the EXAFS formula. We can write

$$\chi(k) = \text{Im } Z(k) \tag{A7}$$

where $Z(k) = X(k) + iY(k)$ and $X(k)$ and $Y(k)$ are real functions. Note that $Y(k) \equiv \chi(k)$.

Experimentally, the errors appear as variations in $\chi(k)$, and how these variations are distributed between A and ϕ is arbitrary. We choose the method of distribution such that

$$A^2\sigma_\phi^2 = \sigma_A^2 \tag{A8}$$

for reasons that will soon become apparent.

Considering eq A7, it is easy to show by differentials that

$$\sigma_A^2 - A^2\sigma_\phi^2 = (\sigma_X^2 - \sigma_Y^2)\cos 2\phi + 2\sigma_{XY}^2 \sin 2\phi$$

$$2A\sigma_{A\phi}^2 = (\sigma_Y^2 - \sigma_X^2)\sin 2\phi + 2\sigma_{XY}^2 \cos 2\phi \tag{A9}$$

$$\sigma_A^2 + A^2\sigma_\phi^2 = \sigma_X^2 + \sigma_Y^2$$

where

$$\sigma_A^2 = \langle((\Delta A)^2\rangle \qquad \sigma_\phi^2 = \langle((\Delta\phi)^2\rangle$$
$$\sigma_X^2 = \langle((\Delta X)^2\rangle \qquad \sigma_Y^2 = \langle((\Delta Y)^2\rangle \qquad \text{(A10)}$$
$$\sigma_{XY}^2 = \langle(\Delta X\Delta Y)\rangle \qquad \sigma_{A\phi}^2 = \langle(\Delta\phi\Delta A)\rangle$$

The $\langle\ \rangle$ symbol denotes an average over the experimental variations. By choosing the relation in eq A8, we note from the first of eq A9 that the left side is zero. In order for this to be true for any value of ϕ

$$\sigma_X^2 = \sigma_Y^2 \qquad \sigma_{XY}^2 = 0 \qquad \text{(A11)}$$

The second equations of eq A9 and A11 then lead to the result that

$$\sigma_{A\phi}^2 = 0 \qquad \text{(A12)}$$

and the third equation of eq A9 then leads to the result that

$$\sigma_A^2 = \sigma_Y^2 = \sigma_X^2 \qquad \text{(A13)}$$

By our choice of eq A8 we eliminate the cross correlation terms $\sigma_{A\phi}^2$ and σ_{XY}^2 and can then easily relate all of the σ^2 to the experimentally determined value of σ_Y^2. Making the substitutions of eq A8 and A13 into eq A4, we find, for χ_ν^2

$$\chi_\nu^2 = \frac{1}{\nu}\sum_i\left[\frac{(A^i)^2(\phi^i_f - \phi^i)^2 + (A^i_f - A^i)^2}{(\sigma^i_Y)^2}\right] \qquad \text{(A14)}$$

It is this quantity that should be minimized to obtain the best fit. Note that the minimization of χ_ν^2 is not the same criterion as is usually employed, namely, minimizing $\sum_i(Y_f^i - Y^i)^2$.

As mentioned in the previous section, the standards used for first-shell oxygen and nitrogen atoms were (Fe_3O)(Gly) and Fe(TIM), respectively. To test how good these standards were for hemerythrin, they were used to fit the data for the three bridged model compounds, (FeOFe)(Bpz), (FeOFe)-(tacn), and (FeOHFe)(Bpz).

The fit used the known parameters of the first-neighbor shell, namely, the number and distance of the nitrogen and oxygen atoms. To optimize the fit, a single Debye–Waller factor for the nitrogen atoms was varied, as were an independent single Debye–Waller factor for the carboxyl oxygen atoms and the E_0 and the Debye–Waller factor for the μ-oxo atom. The Debye–Waller factors were varied because it is expected that they could change somewhat between the standards and the compounds being fit. The μ-oxo atom has a significantly shorter bond (1.8 in place of 2.0 Å) than that of the standard. The charge transfer between the oxygen and the Fe could be different. In addition, the backscattering amplitude of the oxygen atom (like that of all atoms) depends somewhat on the bond distance (Lee & Pendry, 1975; Rehr et al., 1986). Both of these effects can be roughly corrected for by varying E_0. The fitting errors σ_Y^2 are 0.09 for (FeOFe)(Bpz), 0.11 for (FeOFe)(tacn), and 0.08 for (FeOHFe)(Bpz). (FeOFe)(tacn) required a larger E_0 shift than did (FeOFe)(Bpz) and (FeOHFe)(Bpz) for the best fit. The fits for (FeOFe)(Bpz) and (FeOHFe)(Bpz) were correspondingly somewhat better. The fitting errors σ_Y^2 are the mean-square variations between the fitted first-shell $\chi(k)$, obtained by using the $B(k)$ and $\delta(k)$ for oxygen and nitrogen as determined from (Fe_3O)(Gly) and Fe(TIM), respectively, and the known coordination number and distances of the model compounds, and the first shell obtained from the measured $\chi(k)$.

The errors introduced by the experimental measurement were determined by analyzing individual scans separately. Each scan was reduced to its $\chi(k)$ and Fourier transformed, and then the first shell was isolated. The mean-square variation among these scans was calculated. The scans were taken both at different dates and on different beamlines and were repeated under the same conditions. Included in this type of analysis are systematic variations introduced by the experimental setup and in the data analysis. This error is $\langle(\sigma_Y^i)^2\rangle = 0.004$ for met forms of hemerythrin, 0.03 for oxyhemerythrin, and 0.04 for deoxyhemerythrin.

One notes the surprising result that the fitting errors dominate. Note, also that in the literature the fitting errors are usually ignored.

To improve the results, it is necessary to reduce the fitting errors. One way to do this would be to use the compounds (FeOFe)(Bpz), (FeOHFe)(Bpz), and (FeOFe)(tacn) as standards since their environments are more similar to the various forms of hemerythrin than are the employed standards. The difficulty in employing the compounds as standards is that their first shell is a mixture of oxygen and nitrogen at various distances, and it is not possible a priori to separate out each contribution. However, if the compounds are truly close approximations to a given form of hemerythrin, then there exists a method to take advantage of this, namely, subtracting the standard from the unknown. For example, if they are the same, the subtracted signal would be zero and the structure of the unknown is determined to the accuracy of the standard. Even if they are not exactly the same but differ only slightly, the difference would be expected to be small. Fitting this small difference by the original N and O standards would have the same fitting error as shown in Table I, but since the structure of the unknown is that of the similar standard plus the small difference, the percentage error would be much smaller, roughly in the ratio of the difference $\chi(k)$ to the original χ. We took such differences between the first shell of the various forms of hemerythrin and the appropriate bridged model compound. As shown in Figure 3, only the differences of azidometHr minus FeOFe and deoxyHr minus oxyHr were small enough to warrant such an analysis. The results are given in Table II.

Combining the fitting errors and the measurement and analysis errors, we end up with the total errors σ_Y^2 of 0.10 for the met forms of hemerythrin, 0.13 for oxyHr, and 0.12 for deoxyHr. With these values of σ_Y^2 and $N = 7$, the errors in the fitting parameters are determined by varying each parameter independently, keeping the others fixed at the minimum of χ_ν^2 so that χ_ν^2 changes by 1. This procedure assumes that the parameters are independent of one another and correlations between them are small. It is generally agreed that distances and coordination numbers are not strongly correlated. However, E_0 shifts and distances are correlated, while it is usually stated that coordination numbers and Debye–Waller factors are also correlated. In our case the correlation between coordination numbers and reasonable values of the Debye–Waller factor is not very strong because we fit down to low k values of 2.5 Å^{-1}. At such low k values the Debye–Waller factor has little effect, decoupling it from the coordination number. The E_0 shift was significant only for the μ-oxo atom, and our fit to the compounds (FeOFe)(tacn) and (FeOFe)(Bpz) showed that the errors determined by varying χ_ν^2 by 1 are reasonable. We thus feel that the errors determined for the parameters are good estimates.

References

Armstrong, W. H., & Lippard, S. J. (1984) *J. Am. Chem. Soc.* *106*, 4632–4635.

Armstrong, W. H., Spool, A., Papaefthymiou, G. C., Frankel,

R. B., & Lippard S. J. (1984) *J. Am. Chem. Soc. 106*, 3653–3667.
Bevington, P. R. (1969) *Data Reduction and Error Analysis for the Physical Sciences*, McGraw-Hill, New York.
Bunker, B., & Stern, E. A. (1983) *Phys. Rev. B: Condens. Matter 27*, 1017–1027.
Chaudhuri, P., Wieghardt, K., Nuber, B., Weiss, J. (1985) *Angew. Chem., Int. Ed. Engl. 24*, 778–779.
Co, M. S. (1983) Ph.D. Dissertation, Stanford University.
Co, M. S., Hendrickson, W. A., Hodgson, K. O., & Doniach, S. (1983) *J. Am. Chem. Soc. 105*, 1144–1150.
Dawson, J. W., Gray, H. B., Hoenig, H. E., Rossman, G. R., Schredder, J. M., & Wang, R. H. (1972) *Biochemistry 11*, 461–465.
de Waal, D. J., & Wilkins, R. G. (1976) *J. Biol. Chem. 251*, 2339–2343.
Elam, W. T., Stern, E. A., McCallum, J. D., & Sanders-Loehr, J. (1982) *J. Am. Chem. Soc. 104*, 6369–6373.
Elam, W. T., Stern, E. A., McCallum, J. D., & Sanders-Loehr, J. (1983) *J. Am. Chem. Soc. 105*, 1919–1923.
Heald, S. M., Stern, E. A., Bunker, B., Holt, E. M., & Holt, S. L. (1979) *J. Am. Chem. Soc. 101*, 67–73.
Hedman, B., Co, M. S., Armstrong, W. H., Hodgson, K. O., & Lippard, S. J. (1986) *J. Inorg. Chem. 25*, 3708–3711.
Hendrickson, W. A., Co, M. S., Smith, J. L., Hodgson, K. O., & Klippenstein, G. L. (1982) *Proc. Natl. Acad. Sci. U.S.A. 79*, 6255–6259.
Lee, P. A., & Pendry, J. B. (1975) *Phys. Rev. B: Solid State 11*, 2795–2811.
Lee, P. A., Citrin, P. H., Eisenberger, P., & Kincaid, B. M. (1981) *Rev. Mod. Phys. 53*, 769–806.
Loehr, J. S., & Loehr, T. M. (1979) *Adv. Inorg. Biochem. 1*, 235–252.
Maroney, M. J., Kurtz, D. M., Jr., Nocek, J. M., Pearce, L. L., & Que, L., Jr. (1986) *J. Am. Chem. Soc. 108*, 6871–6879.
Petrou, A. L., Armstrong, F. A., Sykes, A. G., Harrington, P. C., & Wilkins, R. G. (1981) *Biochim. Biophys. Acta 670*, 377–384.
Reem, R. C., & Solomon, E. I. (1987) *J. Am. Chem. Soc. 109*, 1216–1226.
Rehr, J. J., Albers, R. C., Natoli, C. R., & Stern, E. A. (1986) *Phys. Rev. B: Conden. Matter 34*, 4350–4353.
Roe, A. L., Schneider, D. J., Mayer, R. J., Pyre, J. W., Widom, J., & Que, L., Jr. (1984) *J. Am. Chem. Soc. 106*, 1676–1681.
Scarrow, R. C., Maroney, M. J., Palmer, S. M., Que, L., Jr., Roe, A. L., Salowe, S. P., & Stubbe, J. (1987) *J. Am. Chem. Soc. 109*, 7857–7864.
Sheriff, S., Hendrickson, W. A., & Smith, J. L. (1987) *J. Mol. Biol. 197*, 273–296.
Shiemke, A. K., Loehr, T. M., & Sanders-Loehr, J. (1984) *J. Am. Chem. Soc. 106*, 4951–4956.
Shiemke, A. K., Loehr, T. M., & Sanders-Loehr, J. (1986) *J. Am. Chem. Soc. 108*, 2437–2443.
Stenkamp, R. E., & Jensen, L. H. (1979) *Adv. Inorg. Biochem. 1*, 219–233.
Stenkamp, R. E., Sieker, L. C., & Jensen, L. H. (1984) *J. Am. Chem. Soc. 106*, 618–622.
Stenkamp, R. E., Sieker, L. C., Jensen, L. H., McCallum, J., & Sanders-Loehr, J. (1985) *Proc. Natl. Acad. Sci. U.S.A. 82*, 713–716.
Stern, E. A. (1974) *Phys. Rev. B: Solid State 10*, 3027–3037.
Stern, E. A., & Heald, S. M. (1983) in *Handbook on Synchrotron Radiation* (Koch, E. E., Ed.) Vol. 1, pp 955–1014, North-Holland, Amsterdam.
Stern, E. A., Sayers, D. E., & Lytle, F. W. (1975) *Phys. Rev. B: Solid State 11*, 4836–4846.
Stern, E. A., Bunker, B., & Heald, S. M. (1980) *Phys. Rev. B: Condens. Matter 21*, 5521–5539.
Toe, B. K., & Lee, P. A. (1979) *J. Am. Chem. Soc. 101*, 2815–2832.
Wieghardt, K., Pohl, K., & Gebert, W. (1985) *Angew. Chem., Int. Ed. Engl. 24*, 778.
Wilkins, R. G., & Harrington, P. C. (1983) *Adv. Inorg. Biochem. 5*, 51–85.